Pharmaceutical Research, Vol. 22, No. 7, July 2005 (© 2005)
DOI: 10.1007/s11095-005-5642-4

Research Paper

Pharmacokinetic–Pharmacodynamic–Efficacy Analysis of Efalizumab in Patients with Moderate to Severe Psoriasis

Chee M. Ng,[1,3] Amita Joshi,[1] Russell L. Dedrick,[2] Marvin R. Garovoy,[2] and Robert J. Bauer[2]

Received March 8, 2005; accepted April 29, 2005

Purpose. Efalizumab is a humanized anti-CD11a monoclonal antibody that demonstrated efficacy in the treatment of patients with psoriasis. The objective of this study was to perform a pharmacokinetic (PK)–pharmacodynamic (PD)–efficacy (E) modeling analysis with intersubject variability assessment to increase our understanding of the interaction of efalizumab with CD11a on T cells and consequent reduction in severity of disease in psoriasis patients.
Methods. A total of 6,329 samples from 240 patients in five Phase I and II clinical studies were used in the analysis. For the analysis, plasma efalizumab concentration was used as the PK measurement, the percent of predose CD11a was used as the PD measurement, and the psoriasis area and severity index was used as the measure of efficacy. A receptor-mediated PK/PD model was developed that describes the dynamic interaction of efalizumab binding with CD11a. In the efficacy model, the rate of psoriasis skin production is directly proportional to the amount of free surface CD11a on T cells, which is offset by the rate of skin healing. An additional CD11a-independent component to psoriasis skin production accounted for incomplete response to efalizumab therapy. A Monte Carlo parametric expectation maximization method implemented in the ADAPT II program was used to obtain the estimate of population parameters and inter- and intrasubject variability.
Results and Conclusions. The final model described the PK/PD/E data in psoriasis patients reasonably well. In addition, simulations using the final model suggested that efalizumab administered less frequently could possibly be more convenient with similar efficacy.

KEY WORDS: anti-CD11a monoclonal IgG1 antibody; efalizumab; Monte Carlo parametric expectation maximization method; population pharmacokinetic, pharmacodynamic, and efficacy model; psoriasis.

INTRODUCTION

Psoriasis is a common chronic inflammatory skin disorder that affects approximately 2% of the world population and results in disability similar to or exceeding that associated with other major illnesses, such as diabetes mellitus and cancer (1,2). It is an incurable autoimmune disease mediated by T lymphocytes and characterized by hyperproliferation of keratinocytes and accumulation of activated T lymphocytes in the epidermis and dermis of psoriatic lesions. A T lymphocyte adhesion molecule, leukocyte-function-associated antigen type 1 (LFA-1), binds with the intercellular adhesion molecule-1, facilitating processes relevant to pathogenesis of psoriasis, including the migration of T lymphocytes from the circulation into dermal and epidermal tissues, with subsequent reactivation (3). Efalizumab, a humanized monoclonal IgG1 antibody, binds to the α subunit of LFA-1 (CD11a), inhibiting the binding of T lymphocytes to endothelial cells, their movement from the circulation into dermal and epidermal tissues, and their activation. The effectiveness of targeting CD11a as a therapeutic approach for psoriasis was demonstrated with efalizumab in clinical studies (4–6). Recently, efalizumab (RAPTIVA®) was approved by the US Food and Drug Administration for treatment of adult patients with chronic moderate and severe psoriasis who are candidates for systemic therapy or phototherapy.

Efalizumab demonstrated dose-dependent nonlinear pharmacokinetics (PK) in patients with psoriasis, which can be explained by its saturable binding to a cell surface receptor, CD11a (7,8). After single intravenous doses, efalizumab clearance decreased from 322 ml/kg/day at 0.1 mg/kg to 6.64 ml/kg/day at 10 mg/kg (7). Efalizumab caused a rapid reduction in the expression of CD11a on circulating lymphocytes, typically to 25–30% of pretreatment levels. The cell surface CD11a remained at this reduced level as long as efalizumab was detectable in the plasma. When efalizumab levels fell below 3 μg/mL, the drug was rapidly cleared from the circulation, and expression of CD11a returned to baseline within 7–10 days (7,8). After a subcutaneous administration of 1.0 mg or 2.0 mg/kg/week for 12 weeks in psoriasis patients, steady-state serum concentrations were achieved by 4 and 8 weeks, respectively. Mean maximum concentrations

[1] Department of Pharmacokinetic and Pharmacodynamic Sciences, Genentech Inc., 1 DNA Way, South San Francisco, California 94080-4990, USA.
[2] XOMA (US) LLC., 2910 Seventh Street, Berkeley, California 94710, USA.
[3] To whom correspondence should be addressed. (e-mail: cheeng@gene.com)

(C_{max}) were 12 and 31 μg/mL, respectively, occurring approximately 2 days after the dose. CD11a expression on T lymphocytes was maximally down-modulated to about 20% of baseline, and CD11a binding sites were >95% saturated (9).

To date, most published pharmacokinetic, pharmacodynamic, and efficacy studies of efalizumab have been descriptive in nature (8,9). A receptor-mediated pharmacokinetic and pharmacodynamic model was developed using data from a single Phase I study to describe the dynamic interaction of efalizumab binding to CD11a, resulting in the removal of efalizumab from the circulation and reduction of surface CD11a of T cells (7). However, the exposure–response relationship of efalizumab was not addressed in the model. This paper expands on the developed receptor-mediated pharmacokinetic and pharmacodynamic model by incorporating data from five Phase I and II studies to develop a pharmacokinetic (PK)–pharmacodynamic (PD)–efficacy (E) model to further increase our understanding of efalizumab interaction with CD11a on T cells and consequent reduction in severity of psoriasis.

MATERIALS AND METHODS

Studies and Patients

Study 1 was a Phase I open-label, single-dose, dose escalation, multicenter study of efalizumab in subjects with a history of moderate to severe plaque psoriasis. Subjects received a single dose of efalizumab at 0.03, 0.1, 0.6, 1, 2, 3, or 10 mg/kg intravenously over 1–3 h. PK samples were collected at predose, 1, 2, 4, 8 h, then 1, 3, 7, 14, 21, 28, 42, and 70 days after start of infusion. PD samples (CD11a levels) were collected at predose, 1, 2, 4, 8 h, then 1, 14, 21, 28, 49, and 70 days after start of infusion. Efficacy was assessed by monitoring changes in clinical signs and symptoms of the disease [psoriasis area and severity index (PASI)] on predose, 7, 14, 21, 28, 42, and 70 days after start of infusion. Data from 30 subjects were included in the analysis.

Study 2 was a Phase I open-label, multiple-dose, dose escalation, multicenter study to determine the safety, pharmacokinetic, and biological activity of efalizumab in subjects with moderate to severe plaque psoriasis. Subjects were to receive intravenous infusions of efalizumab administered either every 2 weeks or once weekly for 7 weeks. Subjects sequentially received the following dose levels in an ascending dose paradigm: 0.1 mg/kg every other week (group A); 0.1 mg/kg weekly (group B); 0.3 mg/kg weekly (group C); 0.3 mg/kg, followed by 0.4 mg/kg a week later, followed by five weekly doses of 0.6 mg/kg (group D); and 0.3 mg/kg, followed by 0.4 mg/kg a week later, followed by 0.6 mg/kg a week later, followed by four weekly doses of 1 mg/kg (group E). Subjects were seen at least weekly during the treatment phase and were followed up for a minimum of 98 days (56 days after the last dose). PK and PD samples were obtained weekly up to day 70. Efficacy was monitored weekly by the PASI. Thirty-nine subjects with PK/PD/E data were included in the analysis.

Study 3 was a Phase I, open-label, single- and multiple-dose, dose escalation, multicenter study to determine the efficacy of subcutaneously administered efalizumab in subjects with moderate to severe plaque psoriasis. Subjects were to receive subcutaneous injections of efalizumab administered as a single dose of 0.3 mg/kg (group A); eight weekly doses of 0.5 mg/kg/week (group B); 0.5 mg/kg, followed by 0.7 mg/kg a week later, then six weekly doses of 1 mg/kg (group C); 0.7 mg/kg, followed by 1 mg/kg a week later, then six weekly doses of 1.5 mg/kg (group D); or 1 mg/kg, followed by 1.5 mg/kg a week later, then six weekly doses of 2 mg/kg (group E). PK samples were obtained on predose, 24, 36, 48, 60, 72 h, then 7, 14, 28, 49, 50, 51, 56, 63, 77, and 91 days after the fist dose. PD samples were collected on predose, 4 h postdosing, then 1, 2, 3, 7, 14, 28, 49, 56, 77, and 91 days after the first dose. PASI was assessed on predose, 14, 21, 28, 42, 56, 77, and 91 days after the first dose. Data from 38 subjects were included in the analysis.

Study 4 was a Phase I, open-label, extended duration, multiple-dose, multicenter study of the effect of efalizumab administered by intravenous or subcutaneous injection to subjects with moderate to severe plaque psoriasis. Subjects were to receive 12 weekly intravenous injections of efalizumab administered at 0.3 mg/kg (group A); intravenous doses of 0.3 mg/kg in the first week, 0.6 mg/kg in the second week, followed by ten weekly doses of 1 mg/kg (group B); subcutaneous injections of 0.7 mg/kg in the first week, followed by 11 weekly doses of 1 mg/kg (group C); subcutaneous injection of 0.7 mg/kg in the first week, followed by 11 weekly doses of 2 mg/kg (group D); subcutaneous injection of 0.7 mg/kg in the first week, followed by 11 weekly doses of 4 mg/kg (group E). Subjects were followed up to day 180. PK samples were collected before and after the last infusion on day 77 and then on days 91, 105, 133, and 180. PD samples were obtained on predose, days 28, 56, 77, 91, 105, 133, and 180. PASI was collected on predose, days 14, 28, 42, 56, 70, 84, 91, 105, 133, and 180. Data from 56 subjects were included in the analysis.

Study 5 was a Phase II, double-blind, multiple-dose, placebo-controlled, multicenter study to evaluate the effect of efalizumab in subjects with moderate to severe plaque psoriasis. Subjects with a minimum PASI of 12 and at least 10% of body surface area (BSA) coverage by psoriasis were randomized to receive eight weekly intravenous infusions of efalizumab or placebo at a 2:1 ratio within each of the two dose groups. The first 31 subjects were randomized to receive either efalizumab 0.1 mg/kg (n = 22) or placebo (n = 9). The remaining subjects were randomized to receive either efalizumab 0.3 mg/kg (n = 75) or placebo (n = 39). PK blood samples were collected before (trough) and after (peak) drug administration at days 0 and 28 and at follow-up visits on days 56 and 70 for the first 60 enrolled patients. PD samples (CD11a) were collected before infusion on days 0, 7, and 28 and at follow-up visits on days 56, 70, and 140. Efficacy was assessed by PASI on predose, days 0, 14, 28, 42, 56, 70, 84, 112, and 140. Data from 77 subjects were included in the analysis.

Efalizumab Assay

A validated immunoassay was developed to measure efalizumab antibody in human plasma (7). Briefly, plasma efalizumab concentrations were determined with the use of an enzyme-linked immunosorbent assay based on the binding of efalizumab to soluble human LFA-1. In the assay, plasma samples were incubated with alkaline phosphate conjugated goat antihuman IgG and substrate p-nitrophenylphosphate. The absorbance at 405 nm was determined using a Vmax

Plate reader (Molecular Devices, Menlo Park, CA). The standard curve ranged from 0.012 to 1,000 ng/ml. The intra- and interassay coefficients of variation were 7 and 11%, respectively.

Flow Cytometric Analysis of CD11a Expression

Phycoerythrin-conjugated anti-CD3 (T cells), anti-CD19 (B cells), and anti-CD56 (NK cells) and fluorescein 5-isothiocyanate-(FITC) conjugated anti-CD11a monoclonal antibody were added to 100-μl aliquots of whole blood (7). Staining reactions were developed at room temperature for 30 min. Erythrocytes were lysed, and cells were analyzed by flow cytometry (Becton Dickinson FACS II, San Jose, CA). Lymphocyte and monocyte populations were identified by forward and side scatter characteristics. The mean fluorescence intensity was measured in arbitrary units in some studies, and absolute binding counts were reported in other studies. Because absolute receptor numbers were not consistently reported, and total number of CD11a positive cells in the body are also unknown, for modeling purposes, in this paper, it was suitable to use the percentage CD11a (%CD11a) level from the mean fluorescence intensity or absolute binding count values, relative to each subject's predose level.

Psoriasis Area and Severity Index

The severity of psoriasis diseases is usually measured using a PASI, which is a composite index indicating the severity of the three main characteristics of psoriatic plaque (erythema, scaling, and thickness) weighted by the amount of coverage of these plaques in the four main body areas (i.e., head, trunk, upper extremities, and lower extremities) (10). PASI scores can range from 0 to 72, with higher scores indicating greater severity and reduction in score representing improvement. PASI is recognized by the US Food and Drug Administration to assess efficacy of psoriasis therapies in clinical trials (11).

Data Set

A total of 7,030 samples from 240 subjects were extracted from the studies. The PASI of 48 subjects after the initiation of concomitant medication was excluded from the analysis. The first efalizumab plasma concentrations to fall below 0.025 μg/ml (level of quantification) after each dose were handled as fixed-point censored observations, and the maximum likelihood was used to fit the model to the censored observations (12). In this case, the likelihood for all the data is maximized with respect to the model parameters, and the likelihood for a censored concentration in particular was taken to be the likelihood that the censored observation is indeed below the level of quantification. All other subsequent efalizumab plasma concentrations below 0.025 μg/ml were excluded from the data analysis. Data points with values much higher and lower than could be physiologically expected for the dose given were excluded from the analysis. These included the CD11a that were very high while efalizumab was still present and neighboring data points were at down-modulated level. A total of 701 points out of 7,030 (10%) were excluded based on the above criteria. Therefore, the final population PK data set consisted of 240 patients with 6,329 samples from five clinical studies. The demographic characteristics of all of the subjects included in the analysis are listed in Table I.

Data were analyzed using a nonlinear mixed-effects modeling method utilizing the Monte Carlo parametric expectation maximization (MCPEM) method implemented in an augmented version of the ADAPT II program (13,14). Briefly, a two-stage hierarchical nonlinear mixed-effect model is used to find the set of mean population parameters μ and population variance matrix Ω that best describes the observed data from m subjects. This was done by maximizing the marginal density of $\boldsymbol{y}$ with respect to μ and Ω by minimizing the following objective function (L):

$$L = -\log\left(p\left(y|\mu,\Omega\right)\right) = \sum_{i=1}^{m} \log\left(\int_{-\infty}^{+\infty} l\left(y_i|\theta\right)h\left(\theta|\mu,\Omega\right)d\theta\right) \tag{1}$$

where $l(y_i \mid \theta)$ is the likelihood or data density for data vector y_i of subject i, given model parameters θ, and $h(\theta \mid \mu, \Omega)$ is the parameter population density for θ, given μ and Ω. It can be shown that if the parameter population density $h(\theta \mid \mu, \Omega)$ is of the form of a multivariate normal distribution with respect to θ, then at the minimum of the objective function, the following relationships are true (15):

$$\mu = \frac{1}{m}\sum_{i=1}^{m}\overline{\theta_i} \tag{2}$$

$$\Omega = \frac{1}{m}\sum_{i=1}^{m}\overline{\Omega_i} \tag{3}$$

where $\overline{\theta_i}$ is the conditional mean θ vector for subject i and $\overline{\Omega_i}$ is the contribution to the population variance from each subject i:

$$\overline{\Omega_i} = \left(\overline{\theta_i} - \mu\right)\left(\overline{\theta_i} - \mu\right)' + \overline{B_i} \tag{4}$$

Table I. Demographic Characteristic of the Patients Included in the Analysis

	Median	Range
Age (years)	45	20–73
Weight (kg)	88.5	52.7–124.2
Body mass index (kg/m^2)[a]	29.7	18.8–46.1
BSA (m^2)[a]	2.01	1.53–2.43
	Number of patient	**Percentage**
Gender		
Male	74	30.8
Female	166	69.2
Race		
Caucasian	209	87.1
African-American	7	2.9
Hispanic	12	5.0
Asian	6	2.5
Others	6	2.5

[a] Obtained from 209 out of 240 patients (87.1%).

where $\overline{B_i}$ is the conditional variance matrix of θ for subject i. Therefore, in the EM algorithm, L is maximized with respect to the population parameters μ and Ω by first evaluating the conditional mean $\overline{\theta_i}$ and conditional variance for each subject using fixed values of μ and Ω (the expectation step E), followed by evaluating updates to μ and Ω using Eqs. (2)–(4) (the maximization step M) (14). In MC-PEM, the Monte Carlo integration method is used to evaluate $\overline{\theta_i}$ and $\overline{B_i}$ during the expectation step (13).

Pharmacokinetic Analysis

A first-order absorption, two-compartment model with both linear and Michaelis–Menten elimination was used to describe the plasma efalizumab concentration data. This model is schematically represented in Fig. 1A. The mass balance equations for this model are given as follows:

$$\frac{dX_{sc}}{dt} = -k_a X_{sc} \tag{6}$$

$$\frac{dX_1}{dt} = -k_{10}X_1 - k_{12}X_1 + k_{21}X_2 - \frac{V_m X_1}{K_{mc}V_c + X_1} + F_a k_a X_{sc} \tag{7}$$

$$\frac{dX_2}{dt} = k_{12}X_1 - k_{21}X_2 \tag{8}$$

where X_{sc} represents the amount of efalizumab in the depot compartment after subcutaneous administration, X_1 represents the amount of efalizumab in the central compartment, X_2 represents the amount of efalizumab in the peripheral compartments, V_m represents the maximal Michaelis–Menten elimination rate, K_{mc} is the Michaelis–Menten constant (the half-maximal concentration of CD11a-mediated efalizumab clearance), k_a is the first-order absorption rate constant, F_a is the fraction bioavailability of efalizumab after subcutaneous administration, k_{10} is the linear elimination rate constant from the central compartment, k_{12} and k_{21} are the intercompartmental rate constants, and V_c is the volume of the central compartment.

Pharmacodynamic Analysis

A receptor-mediated pharmacodynamic model previously developed was used to describe the dynamic interaction of efalizumab to CD11a, resulting in the removal of efalizumab from the circulation and reduction of cell surface CD11a (7). This model is schematically represented in Fig. 1B. To explain the higher than predose CD11a levels that occurred in some subjects after discontinuation of the treatment (rebound phenomenon), surface CD11a on T cells was modeled to cause a negative feedback on production rate of additional CD11a on the cell surface. The differential equations for this model are given as follows:

$$\frac{dX_3}{dt} = X_4 - k_{30}X_3 - \frac{V_{m2}X_3X_1}{K_{mc}V_c + X_1} \tag{9}$$

$$\frac{dX_4}{dt} = k_{off}\left[k_{03max}\left(\frac{K_{mc03}}{K_{mc03} + X_3}\right) - X_4\right] \tag{10}$$

$$\text{Initial condition for } X_3(IC_3) = IC_4/k_{30} \tag{11}$$

$$\text{Initial condition for } X_4(IC_4) = \frac{2k_{03max}}{1 + \sqrt{1 + \frac{4k_{03max}}{K_{mc03}k_{30}}}} \tag{12}$$

X_3 is the total %CD11a on the surface of each T cell, relative to the individual's predose level. The k_{30} represents the first-order rate constant of degradation of %CD11a that is independent of the presence of efalizumab. V_{m2} is the maximal rate of elimination of CD11a in its interaction with efalizumab. K_{mc} represents half-maximal concentration of efalizumab-mediated CD11a elimination. X_4 is the production rate of %CD11a to the T cell surface, in %CD11a/day. The $\left(\frac{K_{mc03}}{K_{mc03}+X_3}\right)$ term represents negative feedback by the total CD11a on the T cell surface on the synthesis of new CD11a. The $k_{off}X_4$ term represents the first-order elimination of CD11a production rate on T cells, and k_{off} is the first-order elimination rate constant of CD11a production rate. K_{mc03} is the half-maximal %CD11a of the negative feedback mechanism. K_{03max} is the maximal production rate of the CD11a to the T cell surface. This model is equivalent to a combination of indirect response models IV and I of Krzyzanski and Jusko (16).

Efficacy Analysis

The severity of the disease was assessed by the PASI score that is assumed to be directly related to the psoriasis skin production. The rate of psoriasis skin production was then modeled to be directly proportional to the amount of free surface CD11a on T cells, which is offset by the rate of skin healing (Fig. 1C). An additional CD11a-independent pathway to psoriasis skin production accounted for lack of complete response to efalizumab therapy. The following differential equations described the model:

$$\frac{dX_5}{dt} = k_{PASI}X_3\left(\frac{K_{mc}V_c}{K_{mc}V_c + X_1}\right) - k_{heal}X_5 + k_{PASI0} \tag{13}$$

$$\text{Initial condition for } X_5(IC_5) = \frac{k_{PASI}IC_3 + k_{PASI0}}{k_{heal}} \tag{14}$$

X_5 is the PASI. The $k_{PASI}X_3\left(\frac{K_{mc}V_c}{K_{mc}V_c+X_1}\right)$ represents the rate of psoriasis skin production, which is directly proportional to the amount of free CD11a on T cells, $X_3\left(\frac{K_{mc}V_c}{K_{mc}V_c+X_1}\right)$. The term $k_{heal}X_5$ is the first-order rate of psoriasis skin healing. k_{PASI0} is the zero-order rate of production of psoriatic skin production that is independent of the amount of free CD11a on T cells.

Interindividual variability among the parameters was assumed to follow a log-normal distribution. A full interindividual variance–covariance matrix was also determined.

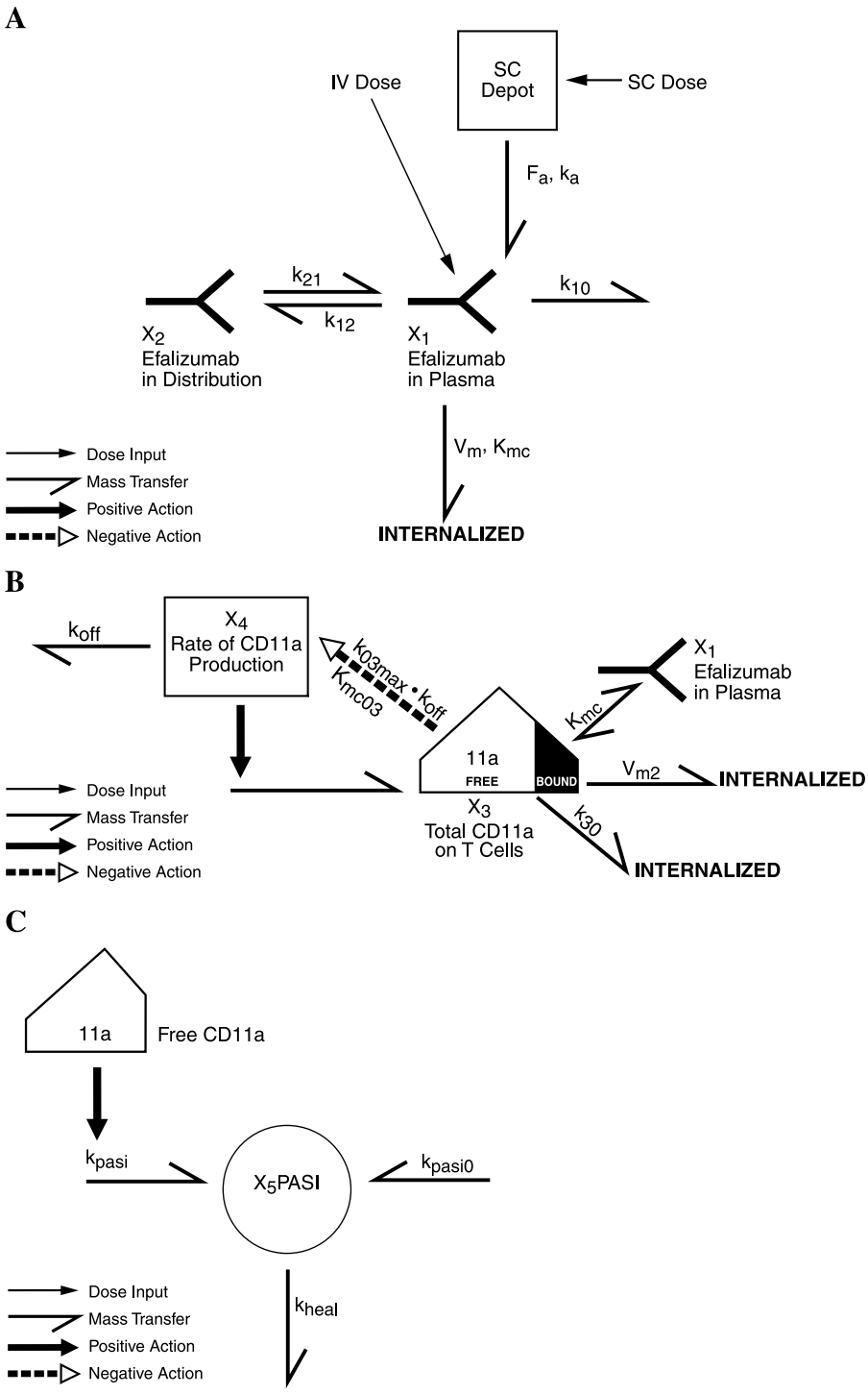

Fig. 1. Schematic representation of pharmacokinetic–pharmacodynamic–efficacy model of efalizumab in psoriasis patients. (A) First-order absorption, two-compartment pharmacokinetic model with linear and nonlinear elimination from the central compartment. (B) Pharmacodynamic model with negative feedback mechanism. (C) Efficacy model with CD11a-dependent and -independent pathway. Parameters are detailed in the text.

A proportional error model was used to describe the intraindividual variability for efalizumab concentration. Intraindividual variability of surface CD11a expression and PASI was modeled with Poisson and constant additive error, respectively. The model was then used to fit the PK/PD/efficacy data simultaneously.

Model Evaluation

The ability of the final PK/PD/E model to describe the observed data was investigated using a simplified posterior model checking method (16–18). The final model, including final fixed-effect and intersubject random-effect parameters, was used to simulate 100 replications of the observed data set. The simulated data were sorted by patients and observation times, and the 97.5th, 95th, 50th (median), 5th, and 2.5th quantiles of the pooled simulated data were calculated for each time point for individual subjects. The percent of observed data that fell within the boundaries of the 97.5th and 2.5th quantiles (95% confidence interval), and 95th and 5th percentiles (90% confidence interval) of the pooled simulated data were determined. The final PK/PD/E model was used to simulate the plasma efalizumab-, CD11a expression-, and percent PASI-time profiles of 1,000 subjects according to the study design of the Phase III, multicenter, randomized, placebo-controlled, double-blind study (4). In addition, 100 trials were simulated, and the percent of subjects who had an improvement of at least 75% in PASI, the primary end point of the study, was computed. The results from the simulated trial were compared with the actual clinical trial results and used to provide evidence that the derived PK/PD/E model accurately described the observed data.

RESULTS

Pharmacokinetic

The plasma concentration-time profile of efalizumab was reasonably described by use of the first-order absorption, two-compartment model with Michaelis–Menten elimination from the central compartment. Figure 2D includes individual predicted *vs.* observed efalizumab concentration data for all patients. Generally, there was good agreement between the individual predicted and the observed plasma concentrations of efalizumab. In addition, diagnostic plots (Fig. 2A) of the final PK model identify no systematic bias. Representation plots of observed and individual predicted plasma concentration-time data for efalizumab in four

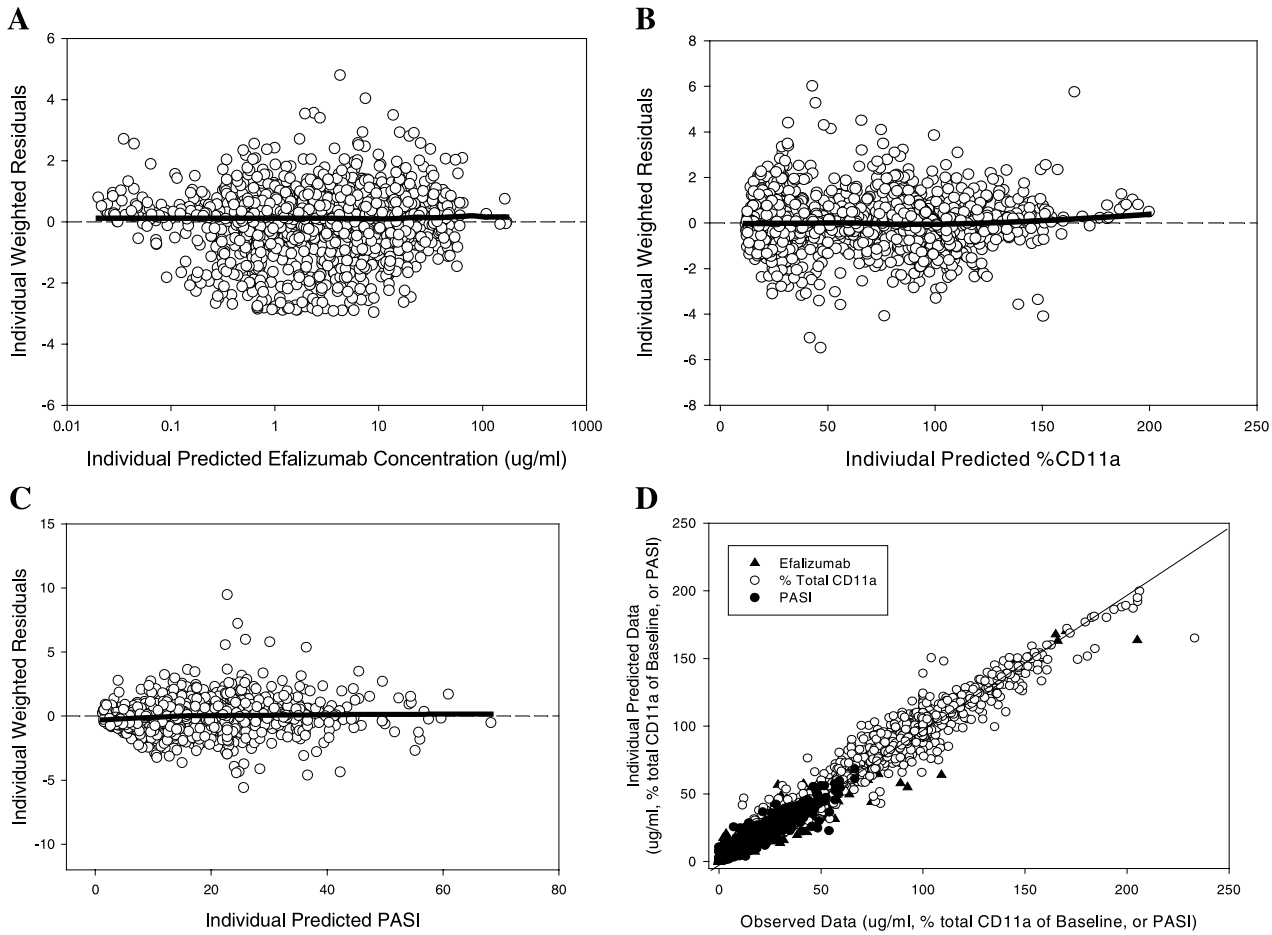

Fig. 2. Diagnostic plots of final pharmacokinetic–pharmacodynamic–efficacy model. Individual weighted residual *vs.* individual predicted (A) efalizumab concentration, (B) %CD11a, and (C) PASI. (D) Individual predicted *vs.* observed pharmacokinetic, pharmacodynamic, and efficacy data. Solid triangle, plasma efalizumab (μg/ml); open circles, %CD11a; solid circles, PASI.

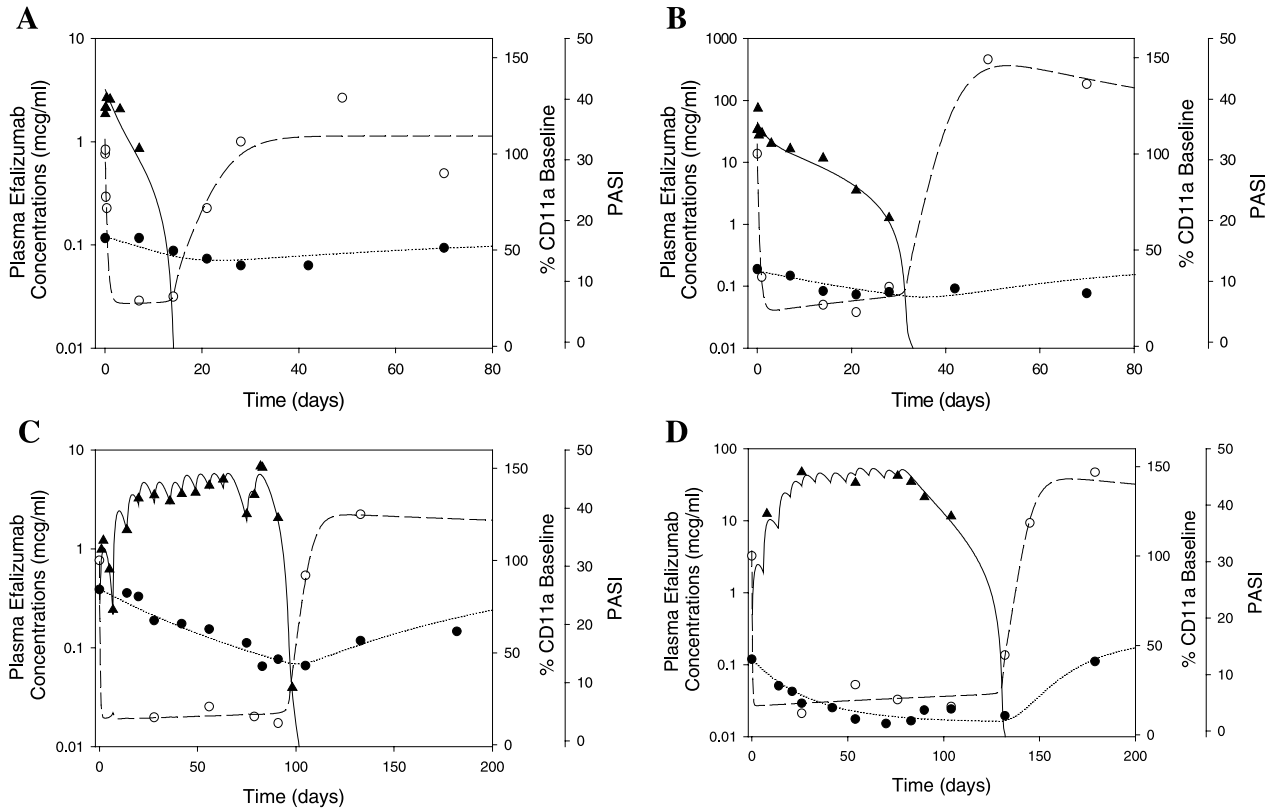

Fig. 3. Individual pharmacokinetic–pharmacodynamic–efficacy profiles from patients who received (A) a single dose of efalizumab at 0.6 mg/kg intravenously, (B) a single dose of efalizumab at 3 mg/kg intravenously, (C) 1 mg/kg weekly dose of efalizumab subcutaneously for 12 weeks, (D) 4 mg/kg weekly dose of efalizumab subcutaneously for 12 weeks. Solid triangle, plasma efalizumab (μg/ml); open circles, %CD11a; solid circles, PASI. Solid, dashed, and dotted lines represent individual predicted plasma efalizumab concentrations, %CD11a baseline, and PASI, respectively.

patients are shown in Fig. 3A–D, again confirming that the proposed model reasonably described the data.

The estimated pharmacokinetic parameters are presented in Table II. The absolute bioavailability of efalizumab after subcutaneous administration F_a was 0.564, and the first-order absorption rate constant was 0.242 day^{-1}. The V_c (64.3 ml/kg) is approximately equal to plasma volume, as is expected for a high molecular weight protein. The typical population values of V_m and K_{mc} were 26.9 μg/kg/day and 0.033 μg/ml, respectively. The nonspecific elimination rate constant from a central compartment k_{10} was 0.114 day^{-1}. The pharmacokinetic parameters and interindividual variability of pharmacokinetic parameters for efalizumab were determined with good precision, with percent standard error of the parameter estimates <22%.

Table II. Final Pharmacokinetic Parameters from the Integrated Pharmacokinetic–Pharmacodynamic–Efficacy Model

Parameters	Population mean (%SE)[a]	Interindividual Variability[b] (%SE)
F_a	0.564 (5.3)	51.2 (13.1)
k_a (day^{-1})	0.242 (9.4)	44.0 (11.6)
k_{10} (day^{-1})	0.114 (5.8)	50.2 (9.5)
k_{12} (day^{-1})	0.097 (21.4)	168 (6.1)
k_{21} (day^{-1})	0.193 (13.0)	95.8 (7.7)
V_c (mL/kg)	64.3 (3.5)	52.0 (9.0)
V_m (μg/kg/day)	26.9 (4.3)	65.0 (8.1)
K_{mc} (μg/mL)	0.033 (20.5)	124 (6.8)
$\sigma_{efalizumab}$[c]	0.359 (1.5)	–

F_a, Fraction bioavailability of efalizumab after subcutaneous administration; k_a, first-order absorption rate; k_{10}, first-order linear elimination rate constant from central compartment; V_m, maximal rate of nonlinear clearance of efalizumab from central compartment; K_{mc}, Michaelis–Menten constant of nonlinear clearance; k_{12} and k_{21}, intercompartmental rate constants.
[a] Percent standard error of the parameter estimate.
[b] Expressed as percent coefficient of variation.
[c] Random residual (intrasubject) variability.

Pharmacodynamics

The pharmacodynamic model for CD11a took into account the down-modulation of CD11a receptor due to its interaction with efalizumab and also the negative feedback action of surface CD11a on its own production rate to account for overshoot effect. As shown in Fig. 3A–D, the model described the observed CD11a-time data reasonably well and was able to capture the overshoot effect (CD11a > 100% baseline). In addition, diagnostic plots (Fig. 2B and D) of the final PD model identify no systematic bias.

The estimated pharmacodynamic parameters are presented in Table III. The pharmacodynamic parameters were determined with good precision, with the highest percent standard error being 22.1%. Interindividual variability in the

Table III. Final Pharmacodynamic and Efficacy Parameters from the Integrated Pharmacokinetic–Pharmacodynamic–Efficacy Model

Parameters	Population mean (%SE)[a]	Interindividual variability[b] (%SE)
Pharmacodynamic		
K_{03max} (%CD11a/day)	334 (9.5)	78.0 (11.4)
K_{mc03} (%CD11a)	15.8 (10.0)	63.9 (13.0)
k_{off} (day^{-1})	0.00154 (22.1)	206 (7.2)
k_{30} (day^{-1})	0.444 (6.6)	66.8 (7.8)
V_{m2} (day^{-1})	2.16 (6.4)	67.7 (9.1)
σ_{CD11a}[c]	0.921 (1.6)	–
Efficacy		
k_{PASI} (PASI/%CD11a/day)	0.00257 (14.7)	102 (7.5)
k_{PASI0} (PASI/day)	0.00851 (46.1)	275 (7.0)
k_{heal} (day^{-1})	0.0142 (14.6)	106 (7.9)
σ_{PASI}[d]	3.32 (1.6)	–

K_{03max}, Maximal rate of CD11a production to T cell surface; K_{mc03}, %CD11a level on T cell surfaces at which K_{03max} is half-inhibited; k_{off}, elimination rate constant of CD11a production rate; k_{30}, first-order rate constant of degradation of CD11a that is independent of the presence efalizumab; V_{m2} is the maximal rate of elimination of CD11a in its interaction with efalizumab; k_{PASI}, CD11a-dependent psoriatic skin production rate; k_{PASI0}, CD11a-independent psoriatic skin production rate; k_{heal}, first-order skin healing rate constant.

[a] Percent standard error of the parameter estimate.

[b] Expressed as percent coefficient of variation.

[c] Residual random (intrasubject) variability of CD11a.

[d] Residual random (intrasubject) variability of PASI.

pharmacodynamic parameter estimates was fairly high, especially for K_{off} (206%). However, the pharmacodynamic parameters for efalizumab were estimated with good precision with the highest percent standard error of 13%.

Efficacy

In the efficacy model, the rate of psoriasis skin production is directly proportional to the amount of free surface CD11a on T cells, which is offset by the rate of skin healing. An additional CD11a-independent component to psoriasis skin production accounted for incomplete response to efalizumab therapy. Again, the model described the observed data well (Figs. 2 and 3A–D). The estimated efficacy parameters are presented in Table III. The k_{PASI} was 0.00257 PASI/%CD11a/day. The k_{PASI0} and k_{heal} were 0.00851 PASI/day and 0.0142 day^{-1}, respectively. The efficacy parameters and their interindividual variability for efalizumab were determined with good precision, with the exception of k_{PASI}, for which the standard error was 46.1%.

Model Evaluation

A simplified posterior predictive model check was used to evaluate the ability of the final model to describe the observed data. The final model was used to simulate 100 replications of the observed data set. The percent of observed data within the 90 and 95% quantile range of the pooled simulated data were 91.1 and 95.0%, respectively. In a subgroup analysis, the percent of observed plasma efalizumab concentrations within the 90 and 95% quantile range of the pooled simulated plasma efalizumab concentrations were 90.0 and 94.0%, respectively. For %CD11a, the percent of observed data within the 90 and 95% quantile range of the pooled simulated data were 90.4 and 94.6%, respectively. The percent of observed PASI within 90 and 95% quantile range of pooled simulated PASI score were 92.9 and 96.4%, respectively. Overall, these results suggest that the model was able to describe and predict the distribution of data reasonably well.

The final PK/PD/efficacy model was used to simulate the plasma efalizumab-, %CD11a expression-, and PASI-time profiles of psoriasis patients according to the study design of the Phase III, multicenter, randomized, placebo-controlled, double-blind study (4). Patients received subcutaneous efalizumab 0.7 mg/kg for the first week, then 1 or 2 mg/kg for 11 weeks. The results from the simulated trials were compared with the actual clinical trial results (Figs. 4 and 5). In general, the simulated trial results agreed with those observed in the actual clinical trial except at the last observed CD11a-time points on day 168. This indicates that our understanding of the pharmacokinetic–pharmacodynamic–efficacy relationships was reasonable enough to predict the time course of plasma efalizumab, %CD11a expression level, and PASI in psoriasis patients treated with efalizumab.

DISCUSSION

In this study, our objective was to develop a mechanism-based PK/PD/E model that describes the plasma efalizumab-, CD11a expression-, and PASI-time profiles for psoriatic patients treated with efalizumab. A receptor-mediated PK/PD model describes the dynamic interaction of efalizumab binding with CD11a. In the efficacy model, the rate of psoriasis skin production is directly proportional to the amount of free surface CD11a on T cells, which is offset by the rate of skin healing. An additional CD11a-independent component to psoriasis skin production accounted for an incomplete response to efalizumab therapy. The final model adequately described the observed data, as illustrated in Figs. 2–4. Therefore, we believe that our objective was achieved. In addition, this article is the first published analysis of population pharmacokinetic/pharmacodynamic/efficacy modeling of efalizumab in patients with moderate to severe psoriasis.

In the PK model, V_c is approximately 64.3 mL/kg, similar to the human plasma volume (45 mL/kg), as is expected for a high molecular weight protein. The saturable elimination of efalizumab is associated with its interaction with CD11a on the surface of white blood cells. This saturable elimination mechanism was modeled using a standard Michaelis–Menten equation with maximal rate of clearance V_m and concentration of half-maximal clearance K_{mc}. According to the model, V_m is considered proportional to the total number of CD11a receptors in the white blood cells which clear efalizumab. The K_{mc} value of 0.033 μg/mL is very similar to the *in vitro* binding affinity of efalizumab for CD11a on lymphocytes (unpublished data). The maximum elimination rate constant of efalizumab from the central

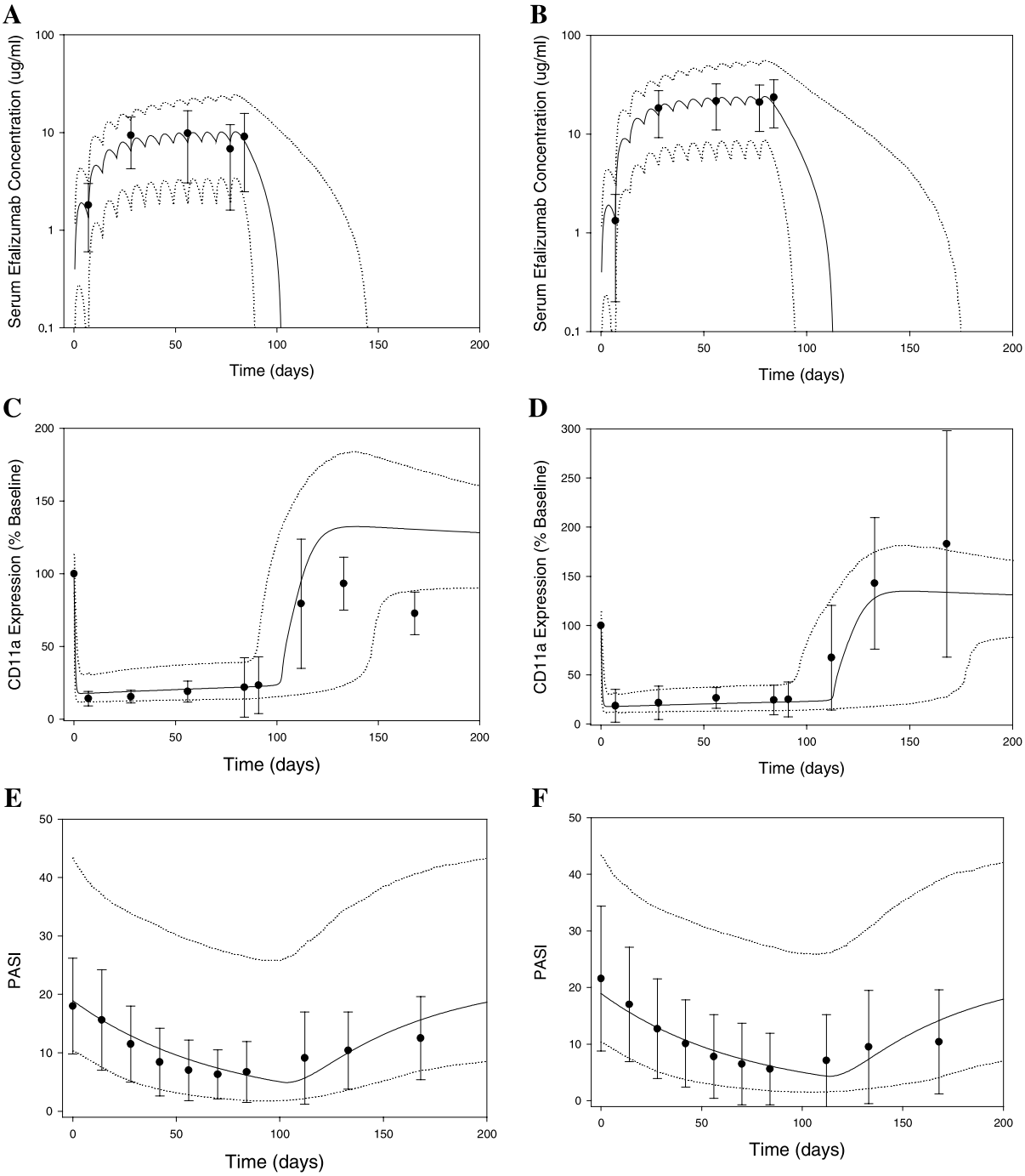

Fig. 4. Comparison of simulated *vs.* actual results of Phase III clinical trial. Left panel (A, C, E): 1 mg/kg/week for 12 weeks. Right panel (B, D, F): 2 mg/kg/week for 12 weeks. Solid circle with error bar, actual results (mean ± SD); solid line, mean values of the simulated results; dotted line, 5 and 95% quantile values of the simulated results. For the actual phase III clinical trial, N = 232 for the 1 mg/kg/week group and N = 243 for the 2 mg/kg/week group. N = 1000 for the simulation trial.

compartment can be obtained at very low concentrations of efalizumab using the following equations:

$$\lim_{X_1 \to 0} \left(\frac{V_m}{K_{mc} V_c + X_1} + k_{10} \right) = \frac{V_m}{K_{mc} V_c} + k_{10} = 12.79 \text{ day}^{-1}$$

This value is about 114 times greater than nonspecific linear elimination rate constant k_{10}, suggesting that the elimination of efalizumab due to CD11a is significant at low efalizumab concentrations. At very high efalizumab concentrations, the nonlinear CD11a-mediated elimination became very small, and the elimination rate of efalizumab approached the value of nonspecific linear elimination rate $k_{10}X_1$. Therefore, the contribution of CD11a-mediated clearance on efalizumab elimination should decrease as the dose increases. This hypothesis was confirmed using the simulation to examine the contribution of CD11a-mediated clearance on efalizumab elimination at different doses. The average percentages of

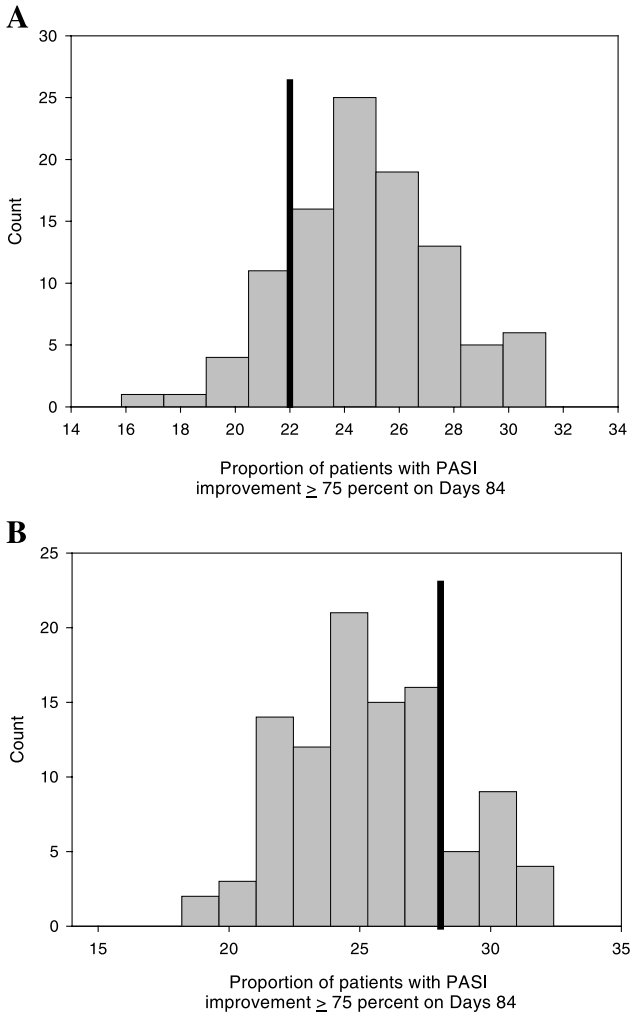

Fig. 5. Observed and predicted proportion of patients with PASI improvement ≥75% on day 84 among patients treated with efalizumab (A) 1 mg/kg/week or (B) 2 mg/kg/week for 12 weeks. Histogram distribution represented results from 100 simulated trials. The vertical line on each histogram represents the result from an actual clinical trial.

total efalizumab dose eliminated by CD11a-mediated nonlinear clearance following a single intravenous dose administration of 0.25, 0.5, 1, 2, and 5 mg/kg to 1,000 simulated subjects were 70.1, 61.1, 49.4, 38.3, and 26.4%, respectively. In our analysis, the pharmacokinetic model with Michaelis–Menten kinetics with rapid receptor binding equilibrium was used. The Michaelis–Menten kinetic model used in our analysis assumed a rapid equilibrium between the binding of antibody to CD11a and dissociation of antibody–CD11a complex and an elimination of the complex from the surface of the cells. This model has been shown to perform equally well with the receptor-mediated disposition model, which assumed slow receptor binding equilibrium (19), and both models could be used to characterize the receptor-mediated disposition of the drugs.

The pharmacodynamic model for CD11a takes into account the down-modulation of CD11a receptors due to its interaction with efalizumab and also the negative feedback action of surface CD11a on its own production rate to account for the overshoot effect. V_{m2} was 2.16 day^{-1}, which differs from the values of V_m in the PK model. This is because the CD11a content on T cells was measured in arbitrary unit of fluorescence intensity and normalized to predose level. Therefore, V_{m2} differs from V_m by an unknown proportional constant. Furthermore, V_m represented all CD11a, including those on non-T cells, that are involved in clearing efalizumab, whereas V_{m2} represented only the clearance rate of CD11a on T cells. Thus, V_{m2} is the coefficient to the term $X_3X_1/(K_{mc} + X_1)$ in the PD equations, which takes into account the amount of CD11a on T cells (X_3) and plasma efalizumab (X_1), whereas V_m is the coefficient to the term $X_1/(K_{mc} + X_1)$ in the PK equations, which assumes that the total CD11a (on T cells plus other cells) that is involved in interacting and eliminating efalizumab is relatively constant, as the degree of CD11a down-modulation on non-T cells tends to be less than those observed on T cells (7). In our previously developed PK/PD model (7), we found that there was no difference in the fit of the data if we used $X_3X_1/(K_{mc} + X_1)$ or $X_1/(K_{mc} + X_1)$ in the PK equations, so we chose the simplest, Michaelis–Menten PK model, for the present analysis.

To account for the overshoot effect of CD11a expression, it was hypothesized that the intracellular process produced CD11a on the T cells at a maximal rate of K_{03max}. The K_{03max} is the production rate where no CD11a was expressed on the surface. This production rate was affected by surface CD11a via a saturable pathway represented by a half-maximal K_{mc03}. The CD11a production rate must be continually replenished to offset the first-order removal rate of CD11a production rate, as represented by k_{off}. Alternatively, the overshoot effect of CD11a expression can be described by the precursor model with negative feedback on the precursor synthesis rate by CD11a level (20). The differential equations for this model are given in the following equations:

$$\frac{dX_4}{dt} = K_{syn}\left(1 - \frac{I_{max}K_{mc03}}{K_{mc03} + X_3}\right) - K_{dp}X_4 - K_{ds}X_4$$

$$\frac{dX_3}{dt} = K_{dp}X_4 - K_{30}X_3$$

where K_{syn} represents zero-order precursor synthesis rate. K_{dp}, K_{ds}, and K_{30} represent first-order rate constant for loss of precursor to total %CD11a, loss of precursor to non-CD11a products, and degradation rate of total %CD11a. I_{max} represents total fractional inhibition by CD11a on precursor production rate. K_{mc03} represents 50% inhibition effect on precursor production rate. The total number of parameters in the model (without drug effects) was six. Therefore, compared to our model with total of four parameters, precursor model with negative feedback required two more parameters, and this may overparameterize the model and may not be supported by the data. Our use of feedback-regulated synthesis was in keeping with the indirect modeling method (15) and had a physiological basis in principles of enzyme kinetics, where an enzyme's activity (as measured by synthesis rate of product) was regulated by negative feedback from its product. In the model, the production rate of the total %CD11a was governed by the total %CD11a on the cell surface. Less total %CD11a on the cell surface increased production rate, and high level of cell surface total %CD11a decreased the production rate of CD11a. Therefore, the

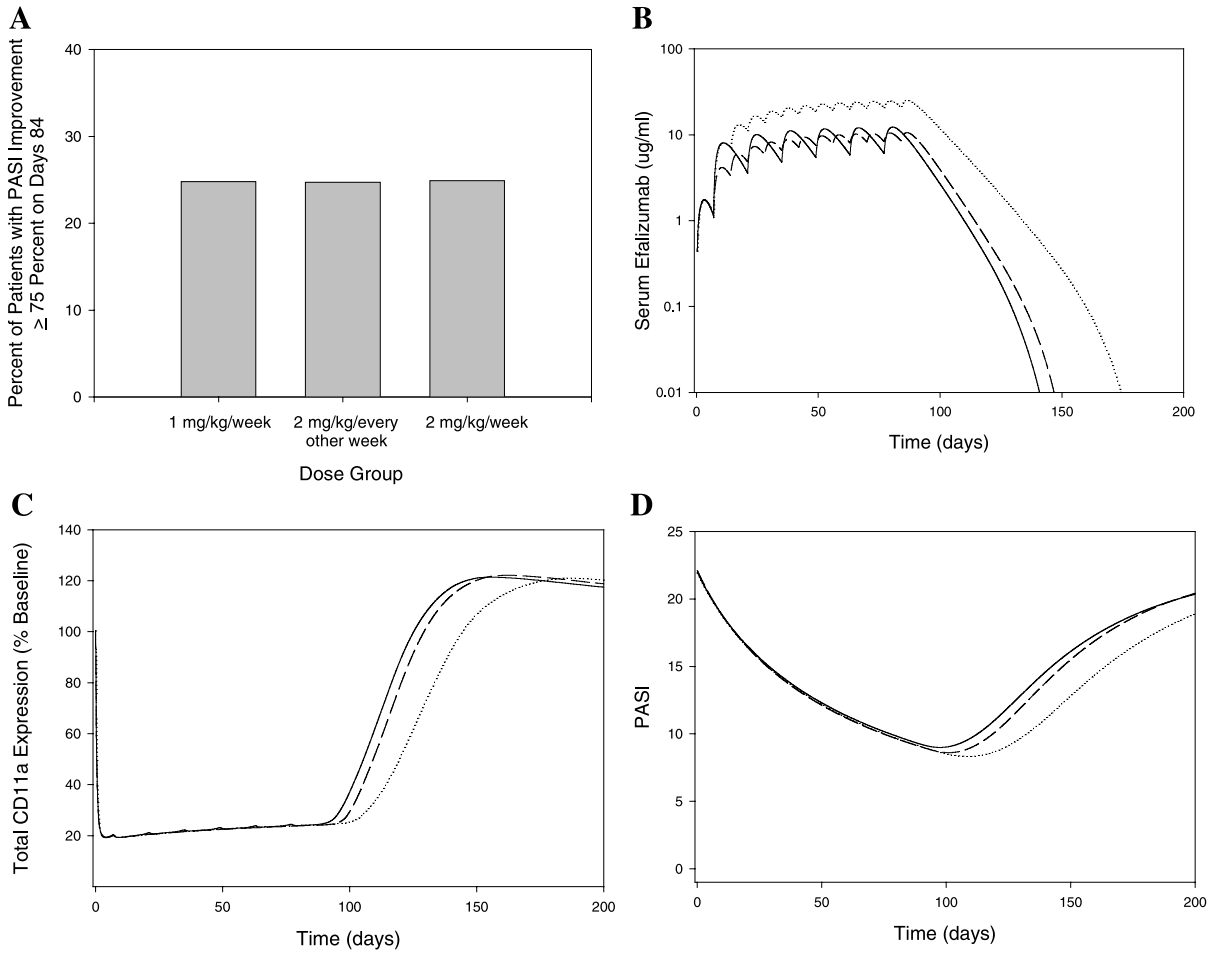

Fig. 6. (A) Model predicted percent of subjects with improvement in PASI at least 75%, and simulated (B) plasma efalizumab-time profile, (C) total CD11a expression-time profile, and (D) PASI score-time profiles for proposed multiple-dose regimens: 0.7 mg/kg for the first week, then 1 mg/kg/week (dashed line), 2 mg/kg every other week (solid line), or 2 mg/kg/week (dotted line).

model with feedback-regulated synthesis instead of the precursor model was used in our analysis.

The final model described the observed CD11a expression-time data reasonably well and able to capture the overshoot effect (CD11a > 100% baseline) (Fig. 3). However, the data set used in this analysis often did not have PD samples that were extensive enough to capture the return of %CD11a to baseline for many of the subjects. More PD data with longer follow-up after termination of efalizumab therapy were needed to better characterize the time course of the CD11a overshoot effect and return of the CD11a to baseline.

Psoriasis is a T-cell-mediated autoimmune disease of the dermis and epidermis characterized by leukocyte infiltration into the skin and impaired skin growth that lead to the development of scaling erythematous plaques (21,22). As described in Materials and Methods, the severity of the psoriasis disease is usually measured using PASI, which is a composite index indicating the extent of psoriasis on four body surface areas and the degree of plaque erythema, scaling, and thickness (10). Therefore, it is reasonable to use PASI as the efficacy endpoint in the model and assume that the PASI is related to the psoriasis skin production. Furthermore, the portion of psoriatic skin production that was dependent on the presence of free %CD11a (not bound to efalizumab) is proportional to the rate constant k_{PASI}. The skin healing process was represented by the first-order rate constant of healing k_{heal}. Thus, when the free CD11a levels declined significantly during efalizumab therapy, psoriatic skin production rate due to interaction of T cells with keratinocytes decreased, and the skin was allowed to heal, leading to reduction of PASI. It was possible for free CD11a to be greater than 100%, and when this happens, psoriatic skin production rate was greater than that occurring at baseline. Therefore, an overshoot in CD11a levels may lead to an overshoot of PASI with a delay in the effect, so that if CD11a overshoot was only transient, rebound in PASI may not be observed. Because not all subjects respond to therapy, or respond partially to efalizumab therapy, psoriatic skin production rate that was independent of free CD11a, k_{PASI0} was included in the efficacy model. One limitation of our efficacy model is lack of a placebo-effect model. The change in PASI with time for patients in the placebo arm of the Phase III trial was about 10% on day 84, comparing to approximately 50% for patients treated with efalizumab, suggesting that a noticeable beneficial placebo effect was observed in the clinical studies (4). However, in our model, we assumed that all the change in PASI score over time after

efalizumab therapy was due to the drug effect. Therefore, the current model overestimated the effect of efalizumab treatment on PASI changes in psoriasis patients. A more realistic efficacy model that incorporated placebo-time effect would be a good next step to better estimate the treatment effect of efalizumab in psoriasis patients (24).

The pharmacokinetic–pharmacodynamic–efficacy model developed here has a broad application to antibodies that target cell-bound receptors, subjected to receptor-mediated clearance, and for which coating and modulation of the receptors are expected to be related to clinical response (25). Despite the nonlinear pharmacokinetics of these agents, the model can be used to describe the time course of the pharmacodynamic effect and efficacy after different dosing regimens.

The final pharmacokinetic–pharmacodynamic–efficacy model was then used to test the hypothesis that less-frequent administration of higher doses would have effects on total CD11a expression and PASI similar to administration of lower doses more frequently. Multiple-dose trials with 1,000 simulated subjects were used to evaluate pharmacokinetics, pharmacodynamics, and efficacy after administration of efalizumab subcutaneously at 0.7 mg/kg for the first week, then 1 mg/kg/week, 2 mg/kg for every other week, or 2 mg/kg/week for 11 weeks. Plots of the percent of subjects with improvement of PASI of at least 75% and mean simulated plasma efalizumab-, total CD11a expression-, and PASI-time profiles with these regimens are shown in Fig. 6. The percent of subjects with PASI improvement of at least 75% were similar. Efalizumab administered at a higher dose but less frequently (2 mg/kg every other week) maximally down-modulated total CD11a expression during the treatment, similar to those observed in subjects who received efalizumab at a lower dose more frequently (1 mg/kg/week). These findings confirm that less-frequent administration of higher doses (2 mg/kg every other week) would have an effect on total CD11a expression and PASI similar to those lower doses given more frequently (1 mg/kg/week). A plan for a clinical study to evaluate the efficacy of efalizumab administered at 2 mg/kg every other week in psoriasis patients is now underway.

In this study, the MCPEM method was used to perform the population analysis of the data. We attempted to fit the data with the model described in this paper using NONMEM (26), but the program would repeatedly terminate without completing the analysis. While NONMEM was used to analyze just the Study 1 data using a simpler PK/PD model as described in our earlier report (7), it nonetheless required repeated restarts to complete the analysis. Compared to NONMEM, the MCPEM method is relatively more stable, requires no restarts even when initial estimates are poor, and is more efficient when analyzing population data using a complex PK/PD model (13).

In summary, a receptor-mediated PK/PD model was developed to describe the dynamic interaction of efalizumab binding with CD11a. In addition, efficacy of efalizumab was modeled with a mechanism-based model. A Monte Carlo parametric expectation maximization method was used to obtain the estimate of population parameters and inter- and intrasubject variability. The final model describes the observed data reasonably well. In addition, simulations using the final model suggested that efalizumab administered less frequently could possibly have similar efficacy, but with more convenience.

ACKNOWLEDGMENTS

We thank Serge Guzy for contributions to implementation of the MCPEM method, and William Jusko for contributions to the rebound of CD11a portion of the model.

REFERENCES

1. E. Christophers. Psoriasis–epidemiology and clinical spectrum. *Clin. Exp. Dermatol.* **26**:314–320 (2001).
2. S. R. Rapp, S. R. Feldman, M. L. Exum, A. B. Fleischer Jr, and D. M. Reboussin. Psoriasis causes as much disability as other major medical diseases. *J. Am. Acad. Dermatol.* **41**:401–407 (1999).
3. J. G. Krueger. The immunologic basis for the treatment of psoriasis with new biologic agents. *J. Am. Acad. Dermatol.* **46**:1–23 (2002).
4. M. Lebwohl, S. K. Tyring, T. K. Hamilton, D. Toth, S. Glazer, N. H. Tawfik, P. Walicke, W. Dummer, X. Wang, M. R. Garovoy, and D. Pariser. A novel targeted T-cell modulator, efalizumab, for plaque psoriasis. *N. Engl. J. Med.* **349**:2004–2013 (2003).
5. K. B. Gordon, K. A. Papp, T. K. Hamilton, P. A. Walicke, W. Dummer, N. Li, B. W. Bresnahan, and A. Menter. Efalizumab for patients with moderate to severe plaque psoriasis: a randomized controlled trial. *JAMA* **290**:3073–3080 (2003).
6. A. Gottlieb, J. G. Krueger, R. Bright, M. Ling, M. Lebwohl, S. Kang, S. Feldman, M. Spellman, K. Wittkowski, H. D. Ochs, P. Jardieu, R. Bauer, M. White, R. Dedrick, and M. Garovoy. Effects of administration of a single dose of a humanized monoclonal antibody to CD11a on the immunobiology and clinical activity of psoriasis. *J. Am. Acad. Dermatol.* **42**:428–435 (2000).
7. R. J. Bauer, R. L. Dedrick, M. L. White, M. J. Murray, and M. R. Garovoy. Population pharmacokinetics and pharmacodynamics of the anti-CD11a antibody hu1124 in human subjects with psoriasis. *J. Pharmacokinet. Biopharm.* **27**:397–420 (1999).
8. A. B. Gottlieb, J. G. Krueger, K. Wittkowski, R. Dedrick, P. A. Walicke, and M. Garovoy. Psoriasis as a model for T-cell-mediated disease: immunobiologic and clinical effects of treatment with multiple doses of efalizumab, an anti-CD11a antibody. *Arch. Dermatol.* **138**:591–600 (2002).
9. D. L. Mortensen, P. A. Walicke, X. Wang, P. Kwon, P. Kuebler, A. B. Gottlieb, J. G. Krueger, C. Leonardi, B. Miller, and A. Joshi. Pharmacokinetics and pharmacodynamics of multiple weekly subcutaneous efalizumab doses in patients with plaque psoriasis. *J. Clin. Pharmcol.* **45**:286–298 (2005).
10. D. M. Ashcroft, A. L. Wan Po, H. C. Williams, and C. E. Griffiths. Clinical measures of disease severity and outcome in psoriasis: a critical appraisal of their quality. *Br. J. Dermatol.* **141**:185–191 (1999).
11. M. A. Menter, G. C. Krueger, S. R. Feldman, and G. D. Weinstein. Psoriasis treatment 2003 at the new millennium: position paper on behalf of the authors. *J. Am. Acad. Dermatol.* **49**:S39–43 (2003).
12. S. L. Beal. Ways to fit a PK model with some data below the quantification limit. *J. Pharmacokinet. Pharmacodyn.* **28**:481–504 (2001).
13. R. J. Bauer and S. Guzy. Monte Carlo parametric expectation maximization (MCPEM) method for analyzing population pharmacokinetic/pharmacodynamic (PK/PD) data. In D. Z. D'Argenio (ed.), *Advanced Methods of Pharmacokinetic and Pharmacodynamic System Analysis,* Vol. 3, Kluwer Academic Publishers, Boston, 2004, pp. 135–163.

14. D. Z. D'Argenio and A Schumitzky. *ADAPT II User's Guide: Pharmacokinetic/Pharmacodynamic System Analysis Software.* Biomedical Simulation Resource, Los Angeles, 1997.
15. A. Schumitzky. EM algorithms and two stage methods in pharmacokinetic population analysis. In D. Z. D'Argenio (ed.), *Advanced Methods of Pharmacokinetic and Pharmacodynamic System Analysis,* Vol. 2, Plenum Press, New York, 1995, pp. 145–160.
16. W. Krzyzanski and W. J. Jusko. Mathematical formalism and characteristics of four basic models of indirect pharmacodynamic responses for drug infusions. *J. Pharmacokinet. Biopharm.* **26**:385–408 (1998).
17. Y. Yano, S. L. Beal, and L. B. Sheiner. Evaluating pharmacokinetic/pharmacodynamic models using the posterior predictive check. *J. Pharmacokinet. Pharmacodyn.* **28**:171–192 (2001).
18. A. Gelman and X. L. Meng. Model checking and model improvement. In W. R. Gilks, S. Richardson, and D. J. Spiegelhalter (eds.), *Markov Chain Monte Carlo in Practice*, Chapman & Hall/CRC, Boca Raton, 1996, pp. 189–202.
19. A. Gelman, J. B. Carlin, H. S. Stern, and D. B. Rubin. *Bayesian Data Analysis*, Chapman & Hall/CRC, Boca Raton, 2004.
20. D. E. Mager and W. J. Jusko. General pharmacokinetic model for drugs exhibiting target-mediated drug disposition. *J. Pharmacokinet. Pharmacodyn.* **28**:507–532 (2001).
21. A. Sharma, W. F. Ebling, and W. J. Jusko. Precursor-dependent indirect pharmacodynamic response model for tolerance and rebound phenomena. *J. Pharm. Sci.* **87**:1577–1584 (1998).
22. A. B. Gottlieb, B. Lifshitz, S. M. Fu, L. Staiano-Coico, C. Y. Wang, and D. M. Carter. Expression of HLA-DR molecules by keratinocytes, and presence of Langerhans cells in the dermal infiltrate of active psoriatic plaques. *J. Exp. Med.* **164**:1013–1028 (1986).
23. S. L. Gottlieb, P. Gilleaudeau, R. Johnson, L. Estes, T. G. Woodworth, A. B. Gottlieb, and J. G. Krueger. Response of psoriasis to a lymphocyte-selective toxin (DAB389IL-2) suggests a primary immune, but not keratinocyte, pathogenic basis. *Nat. Med.* **1**:442–447 (1995).
24. H. Lee, H. C. Kimko, M. Rogge, D. Wang, I. Nestorov, and C. C. Peck. Population pharmacokinetic and pharmacodynamic modeling of etanercept using logistic regression analysis. *Clin. Pharmacol. Ther.* **73**:348–365 (2003).
25. D. R. Mould, C. B. Davis, E. A. Minthorn, D. C. Kwok, M. J. Elliott, M. E. Luggen, and M. C. Totoritis. A population pharmacokinetic–pharmacodynamic analysis of single doses of cleneliximab in patients with rheumatoid arthritis. *Clin. Pharmacol. Ther.* **66**:246–257 (1999).
26. A. J. Boeckmann, L. B. Sheiner, and S. L. Beal. *NONMEM User's Guide*, University of California San Francisco, San Francisco, 1994.